Journal of Applied Mechanics and Technical Physics, Vol. 42, No. 4, pp. 596–602, 2001

UNDULAR JUMP IN OPEN-CHANNEL FLOW OVER A SILL

V. I. Bukreev

UDC 532.59

The paper reports experimental data on a steady flow with a free surface over a rectangular sill at the bottom of a rectangular channel. The paper focuses on the parameter range in which a qualitative change in flow pattern accompanied by formation of an undular jump is observed. It is shown that transition from the bottom state the surface state of head and tail conjugation to occurs when the second critical depth is reached over the downstream edge of the sill. Conditions of transition from a free state to a submerged state of flow over the sill are considered; conditions of validity of the assumption that the first critical depth is reached over the sill are discussed.

The terms "undulations," "undular bore," and "undular jump" are used in hydraulics to describe a transition of the free surface or isopicnical lines or isopicnical lines from one constant value to another that does not occur monotonically or jumpwise but is characterized by gradually damped oscillations. The processes considered are essentially nonlinear.

An undular jump or undular bore can be caused by flow out of a sluice gate or flow over a spillway dam [1], dam break [2, 3], movement of a ship in shallow water [4], landslide of a reservoir shore [5], sudden rise of bottom [6], fall of a body on water [7], nonstationary movement of a container partly filled with a liquid, such as an inclined ship elevator [8], etc. Favre's work [2] arouse interest in these waves, although their particular case — a wavy hydraulic jump — was already described by Bidone [9] and studied by many researchers [1, 10, 11]. Examples of internal-wave undular bores in a stratified liquid are given in [12, 13]. These waves are difficult to analyze theoretically because of their nonlinearity and nonstationarity. In recent studies [14, 15], these waves were calculated rather precisely using the Navier–Stokes equations but only when the solutions remain smooth. Experimental data obtained earlier are given in more detail in [16].

Presnt paper reports results of an experimental study of an undular surface jump formed under certain conditions of steady open flow over a bottom sill of a rectangular channel. Open flows over sills have been extensively studied; the results obtained are given in [1, 11]. Most studies focused on the determination of the discharge coefficient. Undular jumps were explored in [11, 16, 17].

A diagram of the experiment is shown in Fig. 1. A sill of length l and height b was placed at a considerable distance from the entrance of a rectangular channel of width B with zero bottom slope. Previous results show that the shape of the sill edges, especially that of the upstream edge, has a considerable effect on the flow pattern. In the present experiments, the sill edges were sharp. For the steady flow over the sill, the volumetric discharge was Q.

The tail-water depth h_+ measured far from the sill is an important geometrical parameter of the problem (Fig. 1). When h_+ is varied, a number of critical regimes is observed in which the flow pattern changes abruptly. In particular, two flow regimes — free and submerged — are distinguished [1]. In the submerged regime, the value of h_+ influences the drag of the sill, while in the free regime, the drag and the flow pattern upstream of the sill do not depend on h_+. At a certain h_+ and fixed values of the remaining parameters, there is a sharp transition from the bottom state of head and tail conjugation behind the sill to the surface state. The undular jump considered exists only in a limited range of values of h_+. This range can be further divided into the regions of existence of smooth waves and breaking waves. Obtaining new experimental data on the critical regimes is one of the goals of the present work.

Lavrent'ev Institute of Hydrodynamics, Siberian Division, Russian Academy of Sciences, Novosibirsk 630090.
Translated from Prikladnaya Mekhanika i Tekhnicheskaya Fizika, Vol. 42, No. 4, pp. 40–47, July–August, 2001. Original article submitted December 14, 2000.

0021-8944/01/4204-0596 $25.00

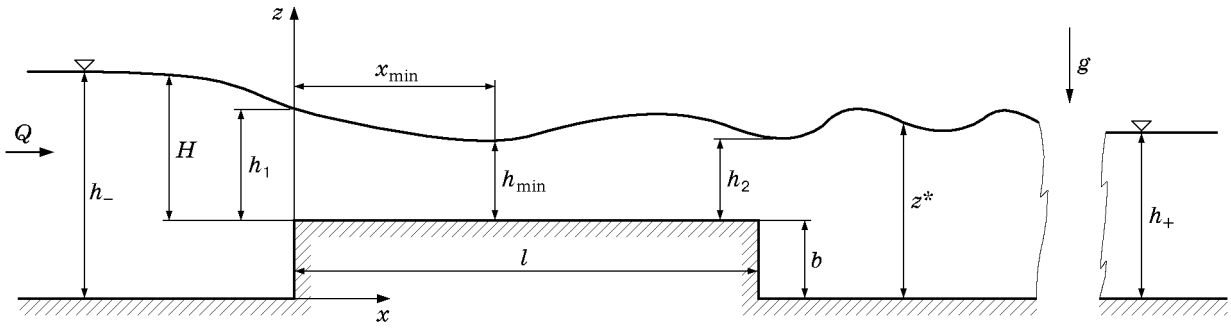

Fig. 1. Diagram of experiment and notation.

The free surface profile $z^*(x)$ was measured with a point gauge and was photo- and video recorded. Particular attention was paid to determining the characteristic values of the functions: $h_1 = z^*(0) - b$, $h_{\min} = z^*(x_{\min}) - b$, and $h_2 = z^*(l) - b$ (Fig. 1). The variance coefficient of the measurement errors for these values did not exceed 2%. Other values of z^* were measured with the same error if the free surface remained smooth. When waves broke and accidental fluctuations z^* occurred, time averaging was performed, and the measurement error reached 5%. We used photo- and video recording to obtain quantitative data on the internal structure of the flow by analyzing trajectories of aluminum particles with sizes smaller than 10 μm introduced into the flow.

Since we further consider the flow kinematics only, in conversion to dimensionless quantities, it is sufficient to choose any two of the specified parameters that contain independently the dimensions of time and length. To this end in hydraulics, it is customary to use the acceleration of gravity g and the head on the sill crest H (Fig. 1), for example, in solving the problem of the discharge capacity of a sill as a spillway, where the discharge Q is an unknown function. This function is expressed in terms of H using the discharge coefficient m, which is determined by the formula [1]

$$Q = mB\sqrt{2g}\, H^{3/2}. \tag{1}$$

According to the goals of the present paper, we choose g and Q as scale variables, and H is one of the unknown functions. This choice was proved by obtaining more universal dependences and more distinct manifestations of certain mechanisms. In this case, the characteristic scales of length and velocity are the critical depth h_* and the critical velocity V_*, which are determined by the formulas [1]

$$h_* = (q^2/g)^{1/3}, \qquad V_* = (gh_*)^{1/2}, \tag{2}$$

where $q = Q/B$ is the discharge intensity. From (1) and (2), we have the following relationship between h_* and H:

$$\frac{1}{\sqrt{2}}\Big(\frac{h_*}{H}\Big)^{3/2} = m.$$

Figure 2 shows typical free surface profiles. We normalized the longitudinal coordinate using the length of the sill, so that the upstream edge of the sill corresponds to $x/l = 0$ and the downstream edge corresponds to $x/l = 1$. The curves in Fig. 2 differ only in the value of the tail-water depth h_+. To analyze the effect of h_+ on the discharge coefficient and the flow upstream of the sill, we used the parameter $\delta = (h_+ - b)/h_*$, called the "downstream submergence ratio" [1]. Let us determine the critical value of this parameter δ_* below which the value of h_+ does not affect the flow pattern upstream of the sill and, particularly, the discharge coefficient. In Fig. 2, curves 1 and 2 presented for $\delta > \delta_*$ and curves 3–5 for $\delta < \delta_*$.

For $\delta \gg \delta_*$ (curve 1 in Fig. 2), waves are generated by both the upstream and downstream edges of the sill; the amplitude and the length of the waves generated by the upstream edge are considerably larger. As values of δ approach δ_*, the influence of waves from the downstream edge and nonlinear effects increases (compare curves 1 and 2 in Fig. 2). Curves 3 and 4 are of considerable interest because $h_{\min}/h_* < 1$ and $\delta > 1$. Thus, the flow is supercritical in a certain section over the sill, and it is subcritical behind the sill. According to the first approximation of the shallow water theory, the transition from supercritical flow to subcritical flow should occur jumpwise (classical hydraulic jump with a roller in its leading part). However, in our case, this transition involved a smooth undular jump.

With further decrease in δ, the undular jump retained smoothness up to a certain value of $\delta_{**} < \delta_*$. For $\delta \simeq \delta_{**}$, its leading edge broke, and for smaller δ, a classical hydraulic jump with a roller on the crest was formed (see curve 5 in Fig. 2). In our experiments, we obtained $\delta_* \simeq 1.33$ and $\delta_{**} \simeq 1.10$.

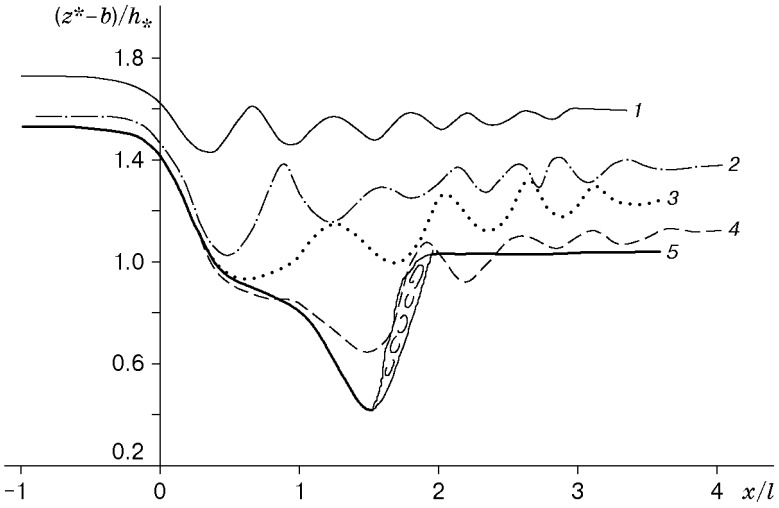

Fig. 2. Examples of wave (curves 1–5) generated by a sill ($h_* = 5.55$ cm, $l/h_* = 5.41$, and $b/h_* = 0.87$): 1) $h_+/h_* = 2.46$, $h_{\min}/h_* = 1.43$, and $H/h_* = 2.59$; 2) $h_+/h_* = 2.25$, $h_{\min}/h_* = 1.04$, and $H/h_* = 2.45$; 3) $h_+/h_* = 2.11$, $h_{\min}/h_* = 0.95$, and $H/h_* = 2.40$; 4) $h_+/h_* = 2.00$, $h_{\min}/h_* = 0.82$, and $H/h_* = 2.40$; 5) $h_+/h_* = 1.91$, $h_{\min}/h_* = 0.80$, and $H/h_* = 2.40$.

When the parameters of the problem were varied, we observed different wave patterns. For example, during transition from an undular jump to a classical hydraulic jump, we observed an unstable regime in which chaotic in time and space perturbations of the free surface behind the roller. These perturbations can be regarded as analogs of the so-called turbulent spots that appear during a laminar–turbulent transition in a boundary layer.

Changes in the wave pattern are due to changes in the internal structure of the flow. Figure 3 shows photographs taken in a narrow vicinity of $\delta = 1$. In the photographs, one can see two vertical white reference lines, which are 10 cm apart in the channel. The value of $\delta = 1$ also proved to be critical because the transition from a surface to bottom state of head and tail conjugation behind the sill occurred at this downstream submergence ratio. In the surface state (Fig. 3a), the liquid flows mainly in the surface jet. In this case, a region of flow separation with thickness comparable to the height of the sill is formed near the bottom of the channel. The length of this region can extend up to a few tens of h_+. In this region, different vortex patterns are formed, which are called coherent structures in terms of the theory of turbulence. The average value of the longitudinal velocity component in this region is relatively small, and particles (for example, of the aluminum powder) that enter this region are rarely brought into the jet.

In the case of the bottom state of conjugation (Fig. 3b), the jet moves toward the bottom and a pair of strong vortices are formed: a roller of a classical hydraulic jump near the free surface and a bottom roller behind the sill. Each of them contains an internal hierarchy of vortices in descending order of size. Observation data taken within a few hours showed that the impurity that entered the bottom roller almost did not flow out of it.

The internal flow structure for transition from a surface state to a bottom state is shown in Fig. 3c.

In the transitional state, the flow depth over the downstream edge of the sill h_2 is of considerable interest. If the critical value of h_2 at which the flow pattern changes is denoted by h_{**} and the corresponding velocity by V_{**}, then from experiments, we have $h_{**} = 0.79h_*$ and $V_{**} = 1.27V_*$. In studies [18, 19] of waves of the undular bore type differently generated, the notion of the second critical propagation speed c_{**} was introduces in addition to the well-known (first) critical propagation speed $c_* = \sqrt{gh}$, where h is the unperturbed liquid depth before a free undular bore. The notion of the second critical propagation speed was introduced because the transition of smooth waves to breaking waves occurs exactly in the neighborhood of c_{**} and not in the neighborhood of c_*, as assumed earlier. The value of c_{**} turned out to be equal to the theoretical limiting propagation speed of solitary waves $c_{**} \simeq 1.3c_*$, which was numerically calculated based on the complete model of potential flow [20].

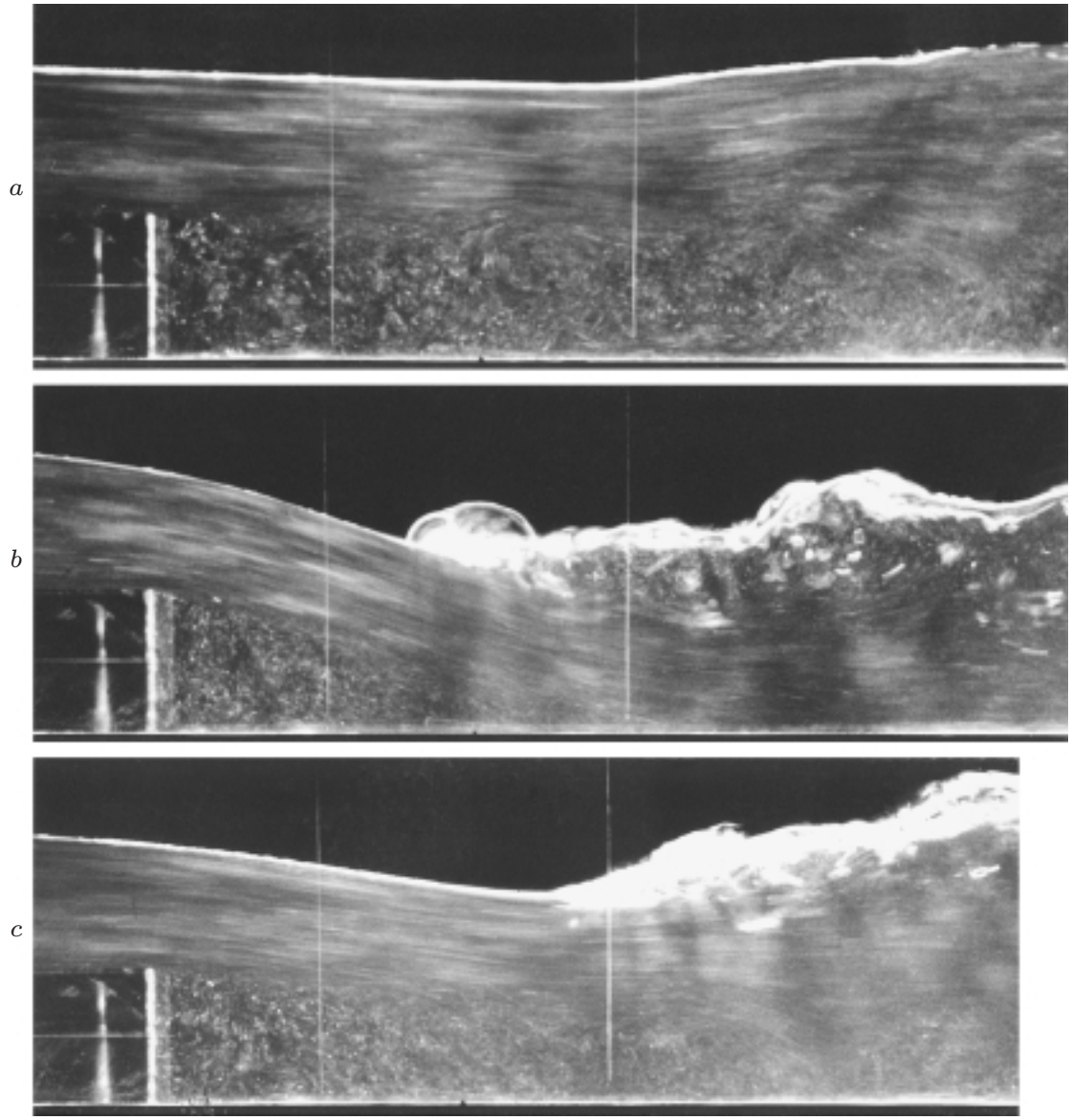

Fig. 3. Internal structure of the flow in surface (a), bottom (b), and transitional (c) states of head and tail conjugation behind the sill ($h_* = 5.55$ cm, $H/h_* = 2.41$, $l/h_* = 5.41$, and $b/h_* = 0.87$) for $\delta = 1.14$ (a), 0.81 (b), and 1.00 (c).

In hydraulics, an analog of c_* is V_*. Since in the relations between V_{**} and V_* and between c_{**} and c_*, the numerical coefficients do not differ greatly from one another, we can expect the second critical velocity V_{**} to be an analog of c_{**} in hydraulic problems. Experimental results obtained showed that there is a range of parameters for the problem considered in which the transition of a surface state of head and tail conjugation to a bottom state occurs when the (cross-section average) velocity of the flow over the downstream edge of the sill reaches the value of the second critical velocity $V_{**} \approx 1.3V_*$ and the second critical depth $h_{**} = q/V_{**}$ establishes.

Applied problems of flow over a sill might be arranged in two groups according to the target aims. The first group of problems seeks to determine the discharge capacity of a sill as a spillway, i.e., the relationship between H and Q. In the second group, one finds the level difference before and after a spillway, i.e., the relationship between $H + b$ and h_+. Results of studying problems of the first group are presented in detail in [1, 11] as empirical formulas. For problems of the second group, insufficient information is available and one has to use additional assumptions, whose field of application is still unknown, such as, for example, the assumption that the first critical depth establishes over a wide sill [1]. Figures 4 and 5 show results of this work for problems of the second group.

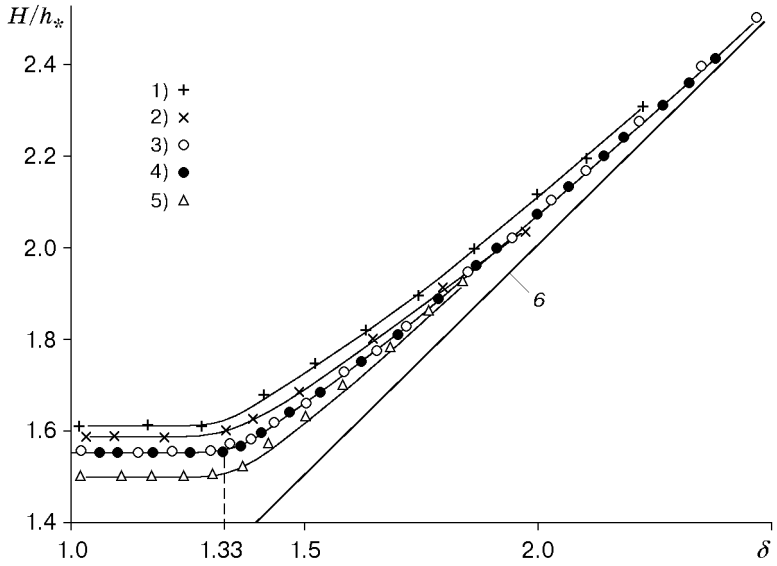

Fig. 4. Head on the sill crest versus discharge and downstream submergence ratio: 1) $h_* = 2.61$ cm, $l/h_* = 11.50$, and $b/h_* = 1.86$; 2) $h_* = 3.09$ cm, $l/h_* = 9.71$, and $b/h_* = 1.57$; 3) $h_* = 4.47$ cm, $l/h_* = 6.71$, and $b/h_* = 1.09$; 4) $h_* = 5.55$ cm, $l/h_* = 5.41$, and $b/h_* = 0.87$; 5) $h_* = 7.24$ cm, $l/h_* = 4.14$, and $b/h_* = 0.67$; 6) $H/h_* = \delta$.

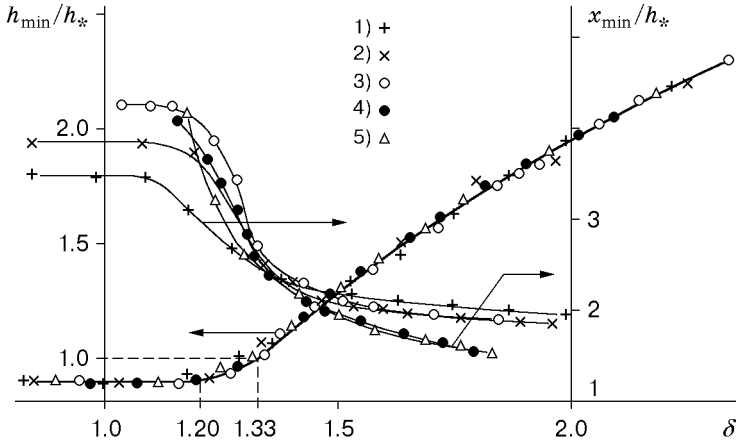

Fig. 5. Minimum depth over the sill and the distance from the depth to the upstream edge of the sill (notation the same as in Fig. 4).

Figure 4 shows curves of H/h_* versus δ. From physical considerations, it follows that $H/h_* \to \delta$ as $\delta \to \infty$. The corresponding asymptote (line 6 in Fig. 4) is the same for different combinations of parameters of the problem. In the studied range of parameters at $\delta > 3$, the deviations from the asymptote did not exceed 2%; with increase in Q, the asymptote was reached faster.

At $\delta = \delta_* \approx 1.33$, we observed an abrupt transition to the asymptotes $H/h_* = \text{const}$, which was associated with transition from submerged flow conditions to free conditions. Values of the constants for these asymptotes depend on the remaining parameters of the problem (see Fig. 4). However, in the studied range of parameters, transition of submerged conditions to free conditions and vice versa occurred for the same value of $\delta \approx 1.33$. This confirms the advantage of choosing h_* as a characteristic length scale.

The data shown in Fig. 5 suggest that there is a range of parameters in which the use of h_* as a characteristic length scale allows us to obtain a universal dependence of the minimum depth over the sill on the downstream submergence ratio. If we use H as a characteristic scale, no universal dependence is obtained. At $\delta < 1.2$, the function $h_{\min}/h_*$ takes a constant asymptotic value that is universal with respect to the parameters of the problem and equal to 0.9.

TABLE 1

Dependence of $z^* - b$ on x

Example 1 ($h_+ = 13.7$ cm)		Example 2 ($h_+ = 12.5$ cm)		Example 3 ($h_+ = 11.7$ cm)		Example 4 ($h_+ = 11.1$ cm)		Example 5 ($h_+ = 10.6$ cm)	
x, cm	$z^* - b$, cm	x, cm	$z^* - b$, cm	x, cm	$z^* - b$, cm	x, cm	$z^* - b$, cm	x, cm	$z^* - b$, cm
−20	14.45	−20	13.65	−20	13.45	−20	13.45	−20	13.45
−12	14.35	−12	13.60	−12	13.35	−12	13.40	−12	13.40
−6	14.25	−6	13.50	−6	13.20	−6	13.25	−6	13.20
0	13.90	0	13.05	0	12.80	0	12.85	0	12.80
6	13.05	6	12.00	6	11.60	6	11.65	6	11.55
11	12.75	12	10.80	12	10.35	12	10.35	12	10.35
15	13.25	15	10.60	18	10.50	18	9.80	15	10.05
20	13.80	22	11.60	25	10.25	24	9.65	19	9.85
24	13.30	27	12.60	30	10.65	28	9.60	24	9.65
28	12.10	30	11.90	37	11.25	30	9.55	30	9.35
30	13.00	37	11.30	44	10.80	40	8.85	34	8.90
37	13.60	43	11.85	50	10.40	45	8.50	38	8.15
42	13.30	48	12.10	56	11.00	50	8.90	42	7.40
46	13.00	54	11.85	61	11.90	53	10.20	45	7.20
50	13.45	60	12.20	66	11.40	57	10.85	49	8.80
54	13.65	64	12.60	71	11.10	62	10.30	51	9.50
60	13.25	70	12.00	76	12.00	66	10.00	53	10.00
66	13.65	77	12.65	79	12.20	70	10.35	55	10.50
71	13.45	81	12.10	82	11.70	77	11.00	60	10.60
75	13.50	86	12.80	86	11.45	84	10.70	65	10.60
79	13.75	92	12.20	92	12.05	88	10.90	70	10.60
84	13.59	100	12.70	97	11.75	93	11.10	80	10.60
88	13.75	110	12.45	100	11.70	100	10.75	90	10.65
95	13.70	120	12.60	110	11.70	110	11.15	100	10.65
110	13.70	130	12.55	120	11.70	115	11.00	110	10.60
120	13.70	140	12.50	140	11.75	120	11.10	120	10.60

Note. The number of an example corresponds to the number of a curve in Fig. 2.

For the function $x_{\min}(\delta)$, universality was not revealed for any characteristic length scales. For normalization to h_* in comparison with normalization to H, curves $x_{\min}/h_*$ (for different values of discharge) intersect at about the same point with coordinates $\delta \approx 1.35$ and $x_{\min}/h_* \approx 2.4$. In the low submergence zone, the function studied also takes constant asymptotic values that depend on discharge.

Thus, our experimental results show that the assumption that the first critical depth h_* establishes over the sill has a limited range of applicability. This assumption is valid only for free flow conditions, i.e., $\delta < 1.33$. The existence of undular jumps requires an even more severe restriction (see Fig. 2). If we require additionally that the coordinate x/l over the sill at which the first critical depth is reached do not depend on the parameters of the problem, the data obtained show that this assumption is valid only at $\delta < 1.2$.

Table 1 shows values of $z^* - b$ versus x to facilitate testing mathematical models.

The author thanks A. V. Gusev and T. V. Krasnoshchekova for their contribution to the derivation of the experimental data.

This work was supported by the Russian Foundation for Fundamental Research (Grant No. 98-01-00750) and the Foundation of Integration Programs of the Siberian Division of the Russian Academy of Sciences (Grant No. 1).

REFERENCES

1. P. G. Kiselev, *Reference Book on Hydraulic Calculations* [in Russian], Gosénergoizdat, Moscow–Leningrad (1957).
2. H. Favre, *Ondes de Translation Dans Les Canaux Decoverts*, Dunod, Paris (1935).
3. R. E. Dreisler, "Comparison of theories and experiments for the hydraulic dam-break wave," *Int. Assoc. Sci. Hydrology*, No. 38, 319–328 (1954).
4. R. C. Ertekin, W. C. Webster, and J. V. Wehausen, "Waves generated by a moving disturbance in a shallow channel of finite width," *J. Fluid Mech.*, **169**, 275–292 (1986).
5. R. L. Wiegel, E. K. Noda, E. M. Kuba, et al., "Water waves generated by landslides in reservoirs," *J. Waterways Harbors Div. Proc. Amer. Soc. Civ. Engrs.*, **96**, No. 2, 307–333 (1970).
6. J. W. Hammack and H. Segur, "The Korteweg–de Vries equation and water waves. Part 2. Comparison with experiments," *J. Fluid Mech.*, **65**, Part 2, 289–314 (1974).
7. V. I. Bukreev and A. V. Gusev, "Gravity waves generated by a body falling on shallow water," *Prikl. Mekh. Tekh. Fiz.*, **37**, No. 2, 90–98 (1996).
8. A. A. Atavin, O. F. Vasil'ev, and V. P. Saptsin, "Hydrodynamic processes during operation of a ship elevator of the Krasnoyarsk waterpower plant," in: *Tr. Gidroproekta*, No. 62 (1978), pp. 100–132.
9. G. Bidone, "Experienses sur le remous et la propagation des ondes," in: *Memorie Reale Accad. Sci.*, **25**, Torin (1820), pp. 21–112.
10. Ven Te Chow, *Open-Channel Hydraulics*, McGraw Hill Book Co, New York, etc. (1959).
11. V. V. Smyslov, *Theory of a Spillway with a Wide Sill* [in Russian], Izd. Akad. Nauk Ukr. SSR, Kiev (1956).
12. V. A. Ivanov and K. V. Konyaev, "Bore on a thermocline," *Izv. Akad. Nauk SSSR*, *Fiz. Atmos. Okeana*, No. 4, 416–423 (1976).
13. P. G. Baines, "Upstream blocking and airflow over mountains," *Annu. Rev. Fluid Mech.*, **19**, 75–97 (1987).
14. C. Marche, P. Beauchemin, and A. El Kaylobi, "Etude numerique et experimentale des ondes secondaires de Favre consecutives à la rupture d'un barrage," *Can. J. Civ. Eng.*, **22**, No. 4, 793–801 (1995).
15. C. M. Lemos, "Higher-order schemes for free surface flows with arbitrary configurations," *Int. J. Numer. Methods Fluids*, **23**, No. 6, 545–566 (1996).
16. J. S. Montes and H. Chanson, "Characteristics of undular hydraulic jumps: experiments and analysis," *J. Hydraul. Eng.*, **124**, No. 2, 192–206 (1998).
17. S. Wu and N. Rajaratnam, "Impinging jet and surface flow regimes at drop," *J. Hydraul. Res.*, **36**, No. 1, 69–74 (1998).
18. V. I. Bukreev and A. V. Gusev, "Waves in a channel ahead of a vertical plate," *Izv. Akad. Nauk, Mekh. Zhidk. Gaza*, No. 1, 82–90 (1999).
19. V. I. Bukreev, E. M. Romanov, and N. P. Turanov, "Breaking of gravity waves in the neighborhood of the second critical speed of their propagation," *Prikl. Mekh. Tekh. Fiz.*, **39**, No. 2, 52–58 (1998).
20. M. S. Longuet-Higgins and J. D. Fenton, "On the mass, momentum, energy, and circulation of a solitary wave. II," *Proc. Roy. Soc., London*, **A340**, 471–493 (1974).